

# ON REAL-TIME ALGORITHMS FOR THE LOCATION SEARCH OF DISCONTINUOUS CONDUCTIVITIES WITH ONE MEASUREMENT

MARTIN HANKE\*

**Abstract.** We discuss, and compare, two simple methods that provide coordinates of a point in the vicinity of one inclusion within some object with homogeneous electrical properties. In the context of nondestructive testing such an inclusion may correspond to a material defect, whereas in medicine this may correspond to a lesion in the brain, to name only two possible applications. Both methods use only one pair of voltage/current measurements on the entire boundary of the object to determine a single pair of coordinates that is considered to be close to the center of the inclusion. The first method has been proposed previously by Kwon, Seo, and Yoon; the second method, called here the effective dipole method, appears to be new. We discuss limitations of the two methods, and derive error bounds for the effective dipole method under realistic assumptions. Finally, we also comment on other methods to localize inclusions.

**Key words.** Inverse conductivity problem, impedance tomography, inclusions

**AMS subject classifications.** 35R30, 65N21

**1. Introduction.** In their paper [14] (see also [8, 13]), Kwon, Seo, and Yoon suggested a real-time algorithm for locating an inclusion in a homogeneous conducting background medium using only one pair of voltage/current measurements on the boundary of the corresponding domain. Here, ‘to locate’ means to construct *one* point in the inclusion or in its close vicinity. Following the title of their paper we will subsequently refer to their method as the *location search method*. Along with convincing numerical results Kwon, Seo, and Yoon provided preliminary theoretical estimates to justify their method for certain ‘restricted cases’ as they say, namely (i) for small disk-shaped inclusions, and (ii) for small contrasts in the conductivity, respectively. They close their introduction with the statement: ‘We expect justifications for less restricted cases to be developed’.

In an attempt to study this method in some broader context, however, we have found that it is sensitive to the values of two free parameters that come with the algorithm. Moreover, an inauspicious choice of these parameters results in a failure of the location search method, except for very special degenerate situations. To be just a little more precise we mention that the location search method is based on zero crossings and local extrema of an auxiliary potential in the exterior of the domain, and according to our analysis below it is important to investigate the near field of this potential and not its far field. In fact, from this point of view the location search method can be seen as a variation of other recurrent ideas of using zero crossings and global extrema of certain boundary measurements to locate inclusions within the body.

We have to admit that our understanding of the location search method is not really complete, but we are in the position to suggest a different, and apparently better, method for locating inclusions, which we shall call the *effective dipole method*. Our approach is based on the fact that the potential constructed by Kwon, Seo, and Yoon is generated by a source supported on the boundary of the inclusion(s). Since any function that is harmonic in the exterior of a bounded domain agrees near infinity up to third order accuracy with a dipole potential, we shall call the corresponding

---

\*Institut für Mathematik, Johannes Gutenberg-Universität Mainz, 55099 Mainz, Germany (hanke@math.uni-mainz.de)

dipole the ‘effective dipole’ of this potential, and use it to locate the inclusion. A simple Fourier analysis of this auxiliary potential yields the location of the effective dipole in a stable way. Numerical results indicate that the effective dipole method performs at least as good as the location search method (with good choice of the free parameters for the latter). From our point of view, however, the behaviour of the effective dipole method is much easier to understand.

Nevertheless, the effective dipole method has its limitations, too, but again these limitations are more transparent: As our method uses only two complex numbers to determine the position and the moment of the effective dipole, lack of uniqueness is an obvious consequence. In fact, counter examples are easy to construct in the more general context of inverse source problems studied in [4], where much more irregular sources are admissible, but in the impedance tomography context considered here we can show that under certain mild restrictions the effective dipole method yields locations that are close to the center of mass of the inclusion.

We like to mention that other, typically iterative methods can and have been used to resolve the inverse conductivity problem with only one measurement, cf., e.g., the results in [1, 6, 7, 10, 12]. Another noniterative approach to deal with this problem can be based on a theory developed recently by Sylvester and his coauthors for inverse scattering problems, i.e., the so-called *convex scattering support* [15]. An application of this idea to the present problem has been worked out in [5], and we refer to Hakula and Hyvönen [3] for a numerical comparison of this approach with our effective dipole method.

The outline of this paper is as follows. In Section 2 we formulate the setting of the underlying problem and give a brief sketch of the location search method from [14] in Section 3. There we also show that the auxiliary potential of Kwon, Seo, and Yoon is the free space electrostatic potential of a certain charge distribution on the boundary of the inclusion. We study in Section 4 the far field of this potential and derive formulae for the effective dipole that generates the same far field asymptotically. As a by-product we can show that the location search method will fail in general when far-field data of this potential are used. Numerical results in Section 5 allow to compare the location search method with the new effective dipole method, before we derive rigorous error bounds for the latter in Section 6. In the final Section 7 we discuss yet another, more intuitive method for locating the inclusion, and point out connections between the various methods. We hope to make evident that the effective dipole method is the most efficient one among all these methods.

**2. Formulation of the problem.** Throughout this paper let  $\Omega$  and  $D$  be bounded, simply connected domains in  $\mathbb{R}^2$  with  $\overline{\Omega} \subset D$ :  $D$  denotes the body of some object under consideration and  $\Omega$  the searched for inclusion within the object. By  $T = \partial D$  and  $\Gamma = \partial\Omega$  we denote the boundaries of the two domains, and by  $\nu$  the normal vectors pointing into the exterior of the respective domains. We usually write  $r = |x|$  for the Euclidean norm of  $x = (x_1, x_2) \in \mathbb{R}^2$ , and  $x^\perp = (x_2, -x_1)$  for the clockwise rotation of  $x$  by the angle  $\pi/2$ .

The inverse conductivity problem we consider in the sequel has the following form: Try to locate the domain  $\Omega$  from the knowledge of the trace  $g = u|_T$  of the weak solution of the formal boundary value problem

$$\nabla \cdot \sigma \nabla u = 0 \quad \text{in } D, \quad \frac{\partial u}{\partial \nu} = f \quad \text{on } T, \quad (2.1)$$

where the conductivity  $\sigma$  is piecewise constant, namely

$$\sigma = \begin{cases} 1 & \text{in } D \setminus \bar{\Omega}, \\ \kappa & \text{in } \Omega, \end{cases} \quad (2.2)$$

for some nonnegative  $\kappa \neq 1$ . The equivalent classical formulation of Problem (2.1), (2.2) is the diffraction problem

$$\begin{aligned} \Delta u &= 0 & \text{in } D \setminus \Gamma, & \quad \frac{\partial u}{\partial \nu} = f & \text{on } T, \\ u^-|_{\Gamma} &= u^+|_{\Gamma}, & \quad \kappa \frac{\partial u^-}{\partial \nu} &= \frac{\partial u^+}{\partial \nu} & \text{on } \Gamma. \end{aligned} \quad (2.3)$$

Superscripts  $+$  and  $-$  specify whether the traces are taken in the exterior or interior of  $\Omega$ , respectively. In order to have a unique and nontrivial solution of (2.1), (2.2), or of (2.3), respectively, we require that

$$0 \neq f \in \mathcal{L}_{\diamond}^2(T) = \left\{ f \in \mathcal{L}^2(T) : \int_T f(y) \, ds(y) = 0 \right\},$$

and normalize the solution  $u$ , which belongs to the standard Sobolev space  $H^1(D)$ , in such a way that its trace  $g$  belongs to  $\mathcal{L}_{\diamond}^2(T)$  as well.

Note that in the so called insulating case, where  $\kappa = 0$ , the diffraction problem (2.3) decouples: The restriction of  $u$  to  $D \setminus \bar{\Omega}$  is given as the solution of a Neumann boundary value problem for the Laplacian with prescribed zero flux across the inner boundary  $\Gamma$ ; then, given  $u|_{D \setminus \bar{\Omega}}$ , this potential is extended to a function  $u \in H^1(D)$  by solving a Dirichlet problem for the Laplacian in  $\Omega$ , using the trace of  $u|_{D \setminus \bar{\Omega}}$  on  $\Gamma$  as Dirichlet data.

For later use we also define the reference potential

$$\Delta u_0 = 0 \quad \text{in } D, \quad \frac{\partial u_0}{\partial \nu} = f \quad \text{on } T, \quad (2.4)$$

and its trace  $g_0 = u_0|_T \in \mathcal{L}_{\diamond}^2(T)$ , which would be measured if no inclusion is present in  $D$ . Occasionally, we refer to  $g$  as the absolute data, and  $g_0 - g$  as the relative data for our problem. With these notations we follow our previous works, e.g., [5] in particular, and apologize to those who are used to quite the reverse notation from [14].

The inverse problem that we are going to consider in this paper is now the following: Locate the inclusion  $\Omega$  from one single pair  $(g, f)$  or  $(g_0 - g, f)$ , respectively, of nontrivial Cauchy data for the diffraction problem (2.3); i.e., determine from these data a point in the vicinity of  $\Omega$ .

**3. The location search method.** To solve this inverse conductivity problem, Kwon, Seo, and Yoon restrict themselves to a boundary current

$$f(y) = a \cdot \nu(y), \quad a \in \mathbb{R}^2, \quad |a| = 1, \quad (3.1)$$

for some fixed vector  $a$ , and use the corresponding boundary potential  $g$  to introduce the auxiliary function

$$H(x) = \int_T \frac{\partial \Phi(x-y)}{\partial \nu(y)} g(y) \, ds(y) - \int_T \Phi(x-y) f(y) \, ds(y), \quad (3.2)$$

where  $x \in \mathbb{R}^2 \setminus \overline{D}$ , and

$$\Phi(x) = \frac{1}{2\pi} \log |x|$$

is the fundamental solution of the Laplace equation. Given  $H$ , which can be evaluated numerically, they determine a root  $\tau = \tau_1$  of

$$h_1(\tau; c_1) = H(c_1 a^\perp + \tau a), \quad \tau \in \mathbb{R}, \quad (3.3)$$

and a local extremum\*  $\tau = \tau_2$  of

$$h_2(\tau; c_2) = H(c_2 a + \tau a^\perp), \quad \tau \in \mathbb{R}.$$

The two real numbers  $c_1$  and  $c_2$  are required to be sufficiently large, for  $H$  is only defined in the exterior of  $D$ , and they are free parameters of the location search method. The appropriate choice of these parameters has not been addressed in [14]; for their numerical examples Kwon, Seo, and Yoon have implemented the method for the unit disk  $D$ , and have chosen  $c_1 = 1.5$  and  $c_2 = -1.5$ , respectively.

The *location search method* is defined to return the point  $x^* = x^*(c_1, c_2) = \tau_1 a + \tau_2 a^\perp$  as ‘location’ of  $\Omega$ , but still, no evidence is provided in [14] that  $\tau_1$  and  $\tau_2$  are well defined.

The potential  $H$  is a combination of a single and a double layer potential, and as such a harmonic function in the exterior of  $D$ . Moreover, because of the constraint  $f \in \mathcal{L}_\diamond^2(T)$ ,  $H$  vanishes at infinity. Using Green’s Theorem and the solution  $u$  of (2.1) we can reformulate (3.2) for  $x \in \mathbb{R}^2 \setminus \overline{D}$  as

$$H(x) = \int_D \nabla_y \Phi(x - y) \cdot \nabla u(y) \, dy - \int_T \Phi(x - y) f(y) \, ds(y),$$

and two more applications of Green’s Theorem in  $\Omega$  and  $D \setminus \overline{\Omega}$ , respectively, yield

$$\begin{aligned} H(x) &= \int_\Gamma \Phi(x - y) \frac{\partial u^-}{\partial \nu}(y) \, ds(y) - \int_\Gamma \Phi(x - y) \frac{\partial u^+}{\partial \nu}(y) \, ds(y) \\ &= \int_\Gamma \Phi(x - y) \varphi(y) \, ds(y), \end{aligned} \quad (3.4)$$

where

$$\varphi = (1 - \kappa) \frac{\partial u^-}{\partial \nu} \Big|_\Gamma \quad (3.5)$$

according to the jump discontinuity (2.3) of the flux of  $u$  across  $\Gamma$ . We prefer the single layer potential representation (3.4) of  $H$  over the corresponding volume integral derived in [14, eq. (2.1)], as it allows a physical interpretation of  $H$  as electrostatic potential of a charge distribution on the boundary of  $\Omega$  with density  $\varphi$  of (3.5). We also note that this representation is valid for any boundary current  $f \in \mathcal{L}_\diamond^2(T)$ , and that it provides a harmonic extension of  $H$  up to the boundary of  $\Omega$ .

We conclude this section by briefly looking at the special case where  $D$  is the unit disk. For doing so, we first apply Green’s Theorem to the second integral in (3.2) –

---

\*whether the extremum of  $h_2$  is a maximum or a minimum depends on the sign of  $\kappa - 1$ , as mentioned in [14], but also on the sign of  $c_2$ .

interpreting  $f$  as the Neumann derivative of the reference potential  $u_0$  from (2.4) – to obtain

$$\begin{aligned} H(x) &= \int_T \frac{\partial \Phi(x-y)}{\partial \nu(y)} g(y) \, ds(y) - \int_T \frac{\partial \Phi(x-y)}{\partial \nu(y)} u_0(y) \, ds(y) \\ &= \int_T \frac{\partial \Phi(x-y)}{\partial \nu(y)} (g(y) - g_0(y)) \, ds(y), \quad x \in \mathbb{R}^2 \setminus \overline{D}, \end{aligned} \quad (3.6)$$

which extends continuously onto  $T$  with

$$H(x) = \int_T \frac{\partial \Phi(x-y)}{\partial \nu(y)} (g(y) - g_0(y)) \, ds(y) - \frac{1}{2} (g(x) - g_0(x))$$

for  $x \in T$ . So far we haven't used that  $D$  is the unit disk, but if this happens to be the case then the kernel  $\partial \Phi(x-y)/\partial \nu(y)$  of the last integral is constant, cf., e.g., Kress [11], and hence, for the unit disk  $D$  the trace of  $H$  on  $T$  coincides with the given relative data – up to a factor of two –, i.e.,

$$H|_T = \frac{1}{2} (g_0 - g), \quad (3.7)$$

as  $g_0$  and  $g$  are both mean free.

**4. Far fields and effective dipoles.** We have investigated numerically the sensitivity of the location search method with respect to its two free parameters  $c_1$  and  $c_2$ . As one outcome of this study we have found that the location  $x^*(c_1, c_2)$  deteriorates when  $|c_1|$  or  $|c_2|$  become large: In general  $x^*(c_1, c_2)$  will fall outside the domain  $D$ , eventually.

To verify this observation we analyze the behavior of  $H(x)$  for large values of  $r = |x|$ . We do so in a slightly more general context, namely, we consider an arbitrary real function  $w$  which is harmonic in the exterior of some open disk  $B_\rho$  around the origin, and which satisfies  $w(x) \rightarrow 0$  as  $|x| \rightarrow \infty$ . Denoting by

$$\hat{x}_t = (\cos t, \sin t), \quad 0 \leq t < 2\pi,$$

the points on the unit circle, we can expand  $w$  in an absolutely converging Fourier series of the form

$$w(r\hat{x}_t) = \sum_{k=-\infty}^{\infty} \alpha_k r^{-|k|} e^{ikt}, \quad r \geq \rho, \quad (4.1)$$

with complex coefficients  $\alpha_k$ ,  $k \in \mathbb{Z}$ . Since  $w$  vanishes at infinity we have  $\alpha_0 = 0$ ; moreover, as  $w$  is real-valued, the Fourier coefficients satisfy  $\alpha_{-k} = \overline{\alpha_k}$  for  $k \in \mathbb{N}$ . Thus, we have

$$w(r\hat{x}_t) = 2(\operatorname{Re} \alpha_1 \cos t - \operatorname{Im} \alpha_1 \sin t) \frac{1}{r} + O\left(\frac{1}{r^2}\right) \quad (4.2)$$

for large values of  $r$ , and this coincides – up to second order – with the field of a dipole

$$D_{z,p}(x) = \frac{1}{2\pi} \frac{(x-z) \cdot p}{|x-z|^2} \quad (4.3)$$

sitting in  $z = 0$  with dipole moment

$$p = 4\pi (\operatorname{Re} \alpha_1, -\operatorname{Im} \alpha_1). \quad (4.4)$$

Note that all the above considerations are fulfilled for  $w = H$ . It follows that near infinity the zero level set  $\mathcal{Z}$  of  $H$  belongs to an arbitrarily narrow sectorial set centered around the vector  $p^\perp$ . As a consequence, if  $x = c_1 a^\perp + \tau_1 a$  denotes the intersection of  $\mathcal{Z}$  with the straight line

$$\Sigma = \{ c_1 a^\perp + \tau a : \tau \in \mathbb{R} \},$$

occurring in (3.3) then  $\tau_1$  is the corresponding root of  $h_1$  and satisfies

$$\tau_1 = \tau_1(c_1) = \frac{a_2 \operatorname{Re} \alpha_1 + a_1 \operatorname{Im} \alpha_1}{a_1 \operatorname{Re} \alpha_1 - a_2 \operatorname{Im} \alpha_1} c_1 + o(c_1), \quad |c_1| \rightarrow \infty,$$

unless  $a = (a_1, a_2)$  of (3.1) happens to be either parallel or orthogonal to  $p$  of (4.4). If  $a$  is orthogonal to  $p$  then  $h_1$  may have no zero at all for  $|c_1|$  sufficiently large. Only when  $a$  is parallel to  $p$  then  $\tau_1(c_1)$  may remain useful when  $|c_1|$  goes to infinity.

Since the above considerations already reveal that the location search method will generically deteriorate when  $|c_1|$  is getting large, we only briefly mention that a similar reasoning with analogous outcome applies when  $|c_2|$  is getting large.

We conclude that the good numerical results presented in [14] rely on the fact that Kwon, Seo, and Yoon consider the potential  $H$  near the boundary of  $D$ , and not its far field. In fact, in their numerical examples  $D$  is the unit disk, and thus, except for a factor of two,  $H$  coincides with the given relative data, cf. (3.7). As a consequence, the location search method is closely related to finding the zeros and local extrema of  $g_0 - g$  on the circle. We emphasize that the latter is a well-known procedure to obtain a first guess about the location of some inclusions, cf., e.g., Lionheart, Polydorides, and Borsic [9], and we will reconsider this issue in Section 7.

Now we return to the analysis of the far field behavior (4.2) of the general potential  $w$ , and incorporate second order information near infinity.

PROPOSITION 4.1. *If  $w$  is given by (4.1) with  $\alpha_1 \neq 0$ , then*

$$w(x) = D_{z,p}(x) + O\left(\frac{1}{|x|^3}\right), \quad |x| \rightarrow \infty, \quad (4.5)$$

if and only if  $p$  is as in (4.4) and

$$z = \left( \operatorname{Re} \frac{\alpha_2}{\alpha_1}, -\operatorname{Im} \frac{\alpha_2}{\alpha_1} \right). \quad (4.6)$$

*Proof.* Expanding  $D_{z,p}$  of (4.3) near infinity we have

$$\begin{aligned} D_{z,p}(r\hat{x}_t) &= \frac{1}{2\pi} (r\hat{x}_t \cdot p - z \cdot p) \left( 1 + 2 \frac{\hat{x}_t \cdot z}{r} + O\left(\frac{1}{r^2}\right) \right) \frac{1}{r^2} \\ &= \frac{1}{2\pi} \left( \frac{\hat{x}_t \cdot p}{r} + \frac{2(\hat{x}_t \cdot p)(\hat{x}_t \cdot z) - z \cdot p}{r^2} + O\left(\frac{1}{r^3}\right) \right). \end{aligned}$$

The first term of this expansion agrees with  $D_{0,p}(r\hat{x}_t)$ , and therefore  $p$  has to be chosen by (4.4) to satisfy (4.5). Turning to the second term of the expansion we write  $p = (p_1, p_2)$  and  $z = (z_1, z_2)$ , and use trigonometric identities to obtain

$$2(\hat{x}_t \cdot p)(\hat{x}_t \cdot z) - z \cdot p = (p_1 z_1 - p_2 z_2) \cos 2t + (p_1 z_2 + p_2 z_1) \sin 2t. \quad (4.7)$$

In complex variables the center  $z$  and the moment  $p$  of the dipole correspond to  $\zeta = z_1 + iz_2$  and  $4\pi\bar{\alpha}_1$ , respectively, cf. (4.4), and thus we can rewrite (4.7) as

$$2(\hat{x}_t \cdot p)(\hat{x}_t \cdot z) - z \cdot p = 4\pi(\operatorname{Re}(\bar{\alpha}_1\zeta) \cos 2t + \operatorname{Im}(\bar{\alpha}_1\zeta) \sin 2t).$$

Comparing this with (4.1) we conclude that (4.5) holds true, if and only if  $p$  is given by (4.4) and

$$2\bar{\alpha}_1\zeta = 2\bar{\alpha}_2,$$

the latter being equivalent to (4.6).  $\square$

It follows that the far field of any potential  $w$  which is harmonic in the exterior of a bounded domain, and which decays like  $1/|x|$  as  $|x| \rightarrow \infty$ , agrees up to third order with the far field of some uniquely defined dipole potential  $D_{z,p}$ . We call  $D_{z,p}$  the *effective dipole* for the potential  $w$ .

**5. The effective dipole method.** As we have already mentioned, the potential  $H$  satisfies the requirements for  $w$  from the previous section if  $\alpha_1 \neq 0$ , and hence, generically,  $H$  agrees near infinity up to third order with the potential of an effective dipole  $D_{z^*,p}$ . Moreover, according to (4.4) and (4.6), the moment  $p$  and the location  $z^*$  of this effective dipole can be readily obtained from a Fourier transform of the values of  $H$  along some circle  $|x| = \rho$  that contains  $D$  in its interior. When  $D$  is the unit disk then we can choose  $\rho = 1$ , and all we need to compute is a fast Fourier transform of the relative data  $g_0 - g$ , cf. (3.7); in the general case we first need to evaluate (3.2), or (3.6), on  $|x| = \rho$  using the trapezoidal rule, say. In any case this method is very easy to implement. As  $H$  is generated by a source located on the boundary of the inclusion  $\Omega$ , cf. (3.4), we can hope that the effective dipole is somehow related to  $\Omega$ , and we therefore propose to use  $z^*$  to locate  $\Omega$ .

This is the *effective dipole method*.

In Figure 5.1 we present numerical results for the location search method and the effective dipole method, respectively, with  $D$  being the unit disk. Each of the four plots shows an inclusion  $\Omega$  within the unit circle, together with its reconstructed locations: In each plot the bullet marks the location computed by the effective dipole method, and the circle depicts the result of the location search method. We have also included the locations (marked by a plus sign) which have been obtained by a third, somewhat ad hoc method, which will be discussed in more detail in Section 7.

For these reconstructions we have used throughout the same boundary current  $f(t) = \sin t$ , corresponding to the choice  $a = (0, 1)$  in (3.1); the conductivity within the inclusion is either  $\kappa = 5$  or  $\kappa = 0$ . Voltage data on the boundary have been computed with a boundary element method, using 768 equidistant grid points on  $T$  and 70 grid points on  $\Gamma$ , respectively. For the implementation of the location search method we have used the same parameters  $c_1 = 1.5$  and  $c_2 = -1.5$  as in [14]; no attempt has been made to optimize these parameters.

As can be seen, the effective dipole method and the ad hoc method give very good results close to the center of the inclusions whereas the results for the location search method are somewhat inferior in two of these examples. (In the example on the upper right of Figure 5.1, taken from [14], all three reconstructions are almost on top of each other).

In a second test series we have run the effective dipole method and the ad hoc method for two representative examples with four different input currents  $f$ , each, cf. Figure 5.2. While three of them are trigonometric current patterns with varying

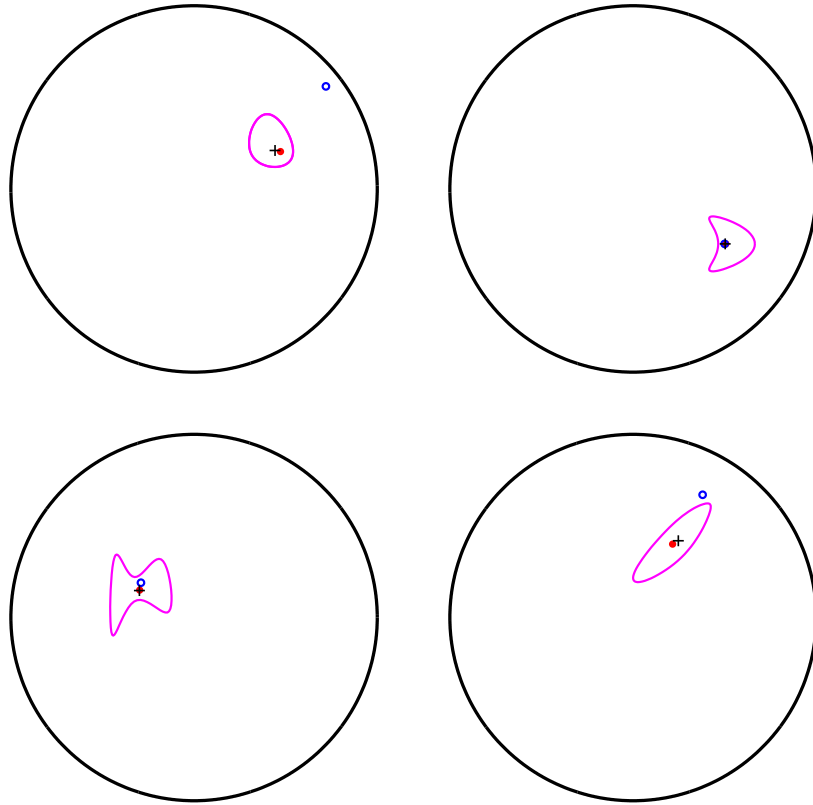


FIG. 5.1. Computed locations of four different inclusions: effective dipole method (bullet) versus the location search method (circle) and the geometric location method (plus signs) of Section 7. The two inclusions in the top row have conductivity  $\kappa = 5$ , inclusions in the bottom row are perfect insulators.

spatial frequencies, the fourth example (‘dipole’) is a localized boundary current obtained from the first 32 terms of the Fourier series of a tangential dipole source located at  $t = \pi/4$ . Only for the nonconvex inclusion one of the computed locations fails to sit within the inclusion. In fact, the locations appear to move towards the boundary of  $\Omega$  with increasing spatial frequency of the current patterns. For the localized boundary current the reconstruction is surprisingly close to the low frequent one. We will partly explain this performance in the following section. In both test series the conductivity  $\kappa$  within the inclusion does not seem to play a prominent role.

Finally, we briefly comment on the influence of noise within the data. As the effective dipole method uses only the first two Fourier coefficients of the potential  $H$  one can expect that the method is pretty stable. On the other hand, as pointed out in [3], for example, in real world situations the amount of noise will rather depend on the magnitude of  $g$  than on  $g_0 - g$ , the latter being much smaller – at least for higher frequencies. Since the relative data  $g_0 - g$  have been used for our numerical experiments it is therefore not surprising to see that the reconstructions with noisy data become worse with increasing frequency of the boundary current, cf. Figure 5.3. In this figure similar reconstructions are shown as in Figure 5.2 (right), but now with 3 % noise in the data relative to the norm of  $g$ . This plot also includes the

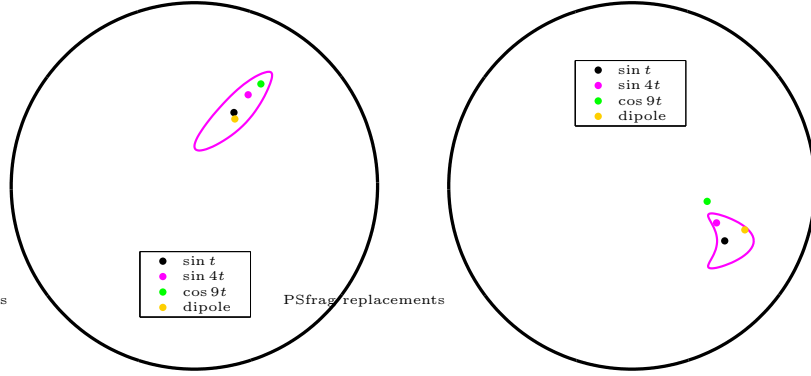


FIG. 5.2. Computed effective dipole locations for different boundary currents; same conductivities as in Figure 5.1.

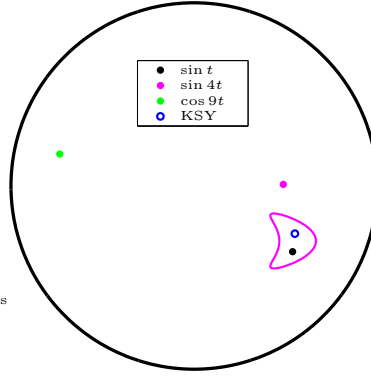


FIG. 5.3. Computed locations for noisy data (3 % noise).

reconstruction of the location search method ('KSY') with input current  $f(t) = \sin t$  for the ease of comparison. It can be seen that only the two reconstructions using this low frequent boundary current are fully stable.

**6. Error bounds for the effective dipole method.** Let  $\zeta$  be the complex number associated with the coordinates (4.6) of the effective dipole  $z^*$  corresponding to the auxiliary potential  $H$ , i.e.,

$$\zeta = \bar{\alpha}_2 / \bar{\alpha}_1, \quad (6.1)$$

where

$$\alpha_k = \frac{1}{2\pi} \rho^k \int_0^{2\pi} H(\rho \hat{x}_t) e^{-ikt} dt, \quad k \in \mathbb{Z}. \quad (6.2)$$

Here, we tacitly assume that  $\alpha_1 \neq 0$ . For later use we emphasize that the location of the effective dipole is independent of rotations of the underlying coordinate system: If we rotate the coordinate system by an angle  $\theta$  counter clockwise, say, then the resulting Fourier coefficients  $\alpha_k$  will be multiplied by  $e^{ik\theta}$ , and hence,  $\zeta$  will be multiplied by  $e^{-i\theta}$ , which corresponds to the same location as before of the effective dipole in the rotated disk.

Inserting (3.4) for  $H$  in (6.2), and using the symmetry of the fundamental solution of the Laplace equation, we first rewrite the Fourier coefficients of  $H$  by

$$\alpha_k = \frac{1}{2\pi} \int_{\Gamma} v_k(x) \varphi(x) \, ds(x), \quad (6.3)$$

where we have introduced, for  $k \in \mathbb{Z}$ , the adjoint potentials

$$v_k(x) = \int_0^{2\pi} \Phi(x - \rho \hat{x}_t) \rho^k e^{-ikt} \, dt = \int_{\partial B_\rho} \Phi(x - y) \psi_k(y) \, ds(y),$$

with

$$\psi_k(\rho \hat{x}_t) = \rho^{k-1} e^{-ikt}, \quad 0 \leq t \leq 2\pi.$$

Using the jump relation of single layer potentials we conclude that  $v_k$  is the (unique) solution of the diffraction problem

$$\begin{aligned} \Delta v_k &= 0 \quad \text{in } \mathbb{R}^2 \setminus \partial B_\rho, & v_k(x) &= o(1) \quad \text{for } |x| \rightarrow \infty, \\ v_k^-(\rho \hat{x}_t) &= v_k^+(\rho \hat{x}_t), & \frac{\partial v_k^+}{\partial \nu}(\rho \hat{x}_t) - \frac{\partial v_k^-}{\partial \nu}(\rho \hat{x}_t) &= \rho^{k-1} e^{-ikt}, \quad 0 \leq t < 2\pi, \end{aligned}$$

and hence,

$$v_k(r \hat{x}_t) = -\frac{1}{2k} \begin{cases} r^k e^{-ikt}, & 0 \leq r < \rho, \\ \rho^{2k} r^{-k} e^{-ikt}, & r \geq \rho. \end{cases} \quad (6.4)$$

For  $k = 1$  and  $k = 2$ , and  $x \in \Gamma \subset D \subset B_\rho$ , this becomes

$$v_1(x) = \frac{-x_1 + ix_2}{2} \quad \text{and} \quad v_2(x) = \frac{x_2^2 - x_1^2 + i 2x_1x_2}{4} \quad (6.5)$$

in terms of the Cartesian coordinates. Inserting this into (6.3) and (6.1) we obtain

$$\zeta = \frac{\int_{\Gamma} ((x_1^2 - x_2^2)/2 + i x_1x_2) \varphi(x) \, ds(x)}{\int_{\Gamma} (x_1 + ix_2) \varphi(x) \, ds(x)}. \quad (6.6)$$

We consider first the denominator of (6.6). Using (3.5) and Green's Theorem we can rewrite

$$\begin{aligned} \int_{\Gamma} (x_1 + ix_2) \varphi(x) \, ds(x) &= (1 - \kappa) \int_{\Omega} \nabla(x_1 + ix_2) \cdot \nabla u(x) \, dx \\ &= (1 - \kappa) \left( \int_{\Omega} \frac{\partial u}{\partial x_1}(x) \, dx + i \int_{\Omega} \frac{\partial u}{\partial x_2}(x) \, dx \right). \end{aligned} \quad (6.7)$$

Similarly we obtain for the numerator of (6.6) the representation

$$\begin{aligned} \int_{\Gamma} ((x_1^2 - x_2^2)/2 + i x_1x_2) \varphi(x) \, ds(x) &= (1 - \kappa) \int_{\Omega} (x_1 + ix_2, -x_2 + ix_1) \cdot \nabla u(x) \, dx \\ &= (1 - \kappa) \left( \int_{\Omega} (x_1, -x_2) \cdot \nabla u(x) \, dx + i \int_{\Omega} (x_2, x_1) \cdot \nabla u(x) \, dx \right). \end{aligned}$$

Expanding (6.6) by the complex conjugate of (6.7) we eventually find that the coordinates of  $z^* = (z_1, z_2)$ , i.e., the real and imaginary parts of  $\zeta$  are given by

$$z_1 = \left( \int_{\Omega} x_1 \frac{\partial u}{\partial x_1} dx \int_{\Omega} \frac{\partial u}{\partial x_1} dx + \int_{\Omega} x_1 \frac{\partial u}{\partial x_2} dx \int_{\Omega} \frac{\partial u}{\partial x_2} dx \right. \\ \left. - \int_{\Omega} x_2 \frac{\partial u}{\partial x_2} dx \int_{\Omega} \frac{\partial u}{\partial x_1} dx + \int_{\Omega} x_2 \frac{\partial u}{\partial x_1} dx \int_{\Omega} \frac{\partial u}{\partial x_2} dx \right) / M$$

and

$$z_2 = \left( \int_{\Omega} x_1 \frac{\partial u}{\partial x_2} dx \int_{\Omega} \frac{\partial u}{\partial x_1} dx - \int_{\Omega} x_1 \frac{\partial u}{\partial x_1} dx \int_{\Omega} \frac{\partial u}{\partial x_2} dx \right. \\ \left. + \int_{\Omega} x_2 \frac{\partial u}{\partial x_1} dx \int_{\Omega} \frac{\partial u}{\partial x_1} dx + \int_{\Omega} x_2 \frac{\partial u}{\partial x_2} dx \int_{\Omega} \frac{\partial u}{\partial x_2} dx \right) / M,$$

where

$$M = \left( \int_{\Omega} \frac{\partial u}{\partial x_1} dx \right)^2 + \left( \int_{\Omega} \frac{\partial u}{\partial x_2} dx \right)^2. \quad (6.8)$$

Reordering terms, this can be rewritten in the following way:

$$z^* = \int_{\Omega} x c(x) dx + \int_{\Omega} x^{\perp} d(x) dx, \quad (6.9)$$

where

$$c(x) = \frac{\partial u}{\partial x_1}(x) \frac{1}{M} \int_{\Omega} \frac{\partial u}{\partial x_1} dy + \frac{\partial u}{\partial x_2}(x) \frac{1}{M} \int_{\Omega} \frac{\partial u}{\partial x_2} dy \quad (6.10)$$

and

$$d(x) = \frac{\partial u}{\partial x_1}(x) \frac{1}{M} \int_{\Omega} \frac{\partial u}{\partial x_2} dy - \frac{\partial u}{\partial x_2}(x) \frac{1}{M} \int_{\Omega} \frac{\partial u}{\partial x_1} dy. \quad (6.11)$$

Note that

$$\int_{\Omega} c(x) dx = 1 \quad \text{and} \quad \int_{\Omega} d(x) dx = 0. \quad (6.12)$$

As a consequence of (6.10) and (6.11), if we adopt at this point the motivating assumption from [14], namely that  $\nabla u = (a_1, a_2) \in \mathbb{R}^2$  is constant within  $\Omega$ , then  $d = 0$  and  $c = 1/|\Omega|$  are also constant ( $|\Omega|$  denotes the area of  $\Omega$ ), and hence,  $z^*$  is the center of mass  $\bar{x}$  of  $\Omega$ . Moreover, we can relax this assumption to obtain error bounds for  $z^* - \bar{x}$ . To this end, we first introduce the mean of the gradient over  $\Omega$ , i.e.,

$$\bar{g} = \frac{1}{|\Omega|} \int_{\Omega} \nabla u(y) dy, \quad (6.13)$$

and conclude from (6.7) that  $\alpha_1 \neq 0$ , if and only if  $\bar{g} \neq 0$ .

**THEOREM 6.1.** *Denote by  $\bar{x}$  the center of mass of  $\Omega$ , and assume that the effective dipole  $z^*$  of  $H$  is well defined, i.e., that  $\bar{g}$  of (6.13) is nonzero. If*

$$\frac{|\nabla u(x) - \bar{g}|}{|\bar{g}|} \leq \epsilon \quad (6.14)$$

for some  $\epsilon > 0$  and all  $x \in \Omega$ , then we have

$$|z^* - \bar{x}| \leq \omega \epsilon,$$

where  $\omega = \int_{\Omega} |x| dx / |\Omega|$  is the mean absolute value within  $\Omega$ .

*Proof.* With  $\bar{g} = (g_1, g_2)$  we can rewrite

$$c(x) = \frac{|\Omega|}{M} \left( g_1 \frac{\partial u}{\partial x_1}(x) + g_2 \frac{\partial u}{\partial x_2}(x) \right)$$

and

$$\frac{1}{|\Omega|} = \frac{|\Omega|}{M} (g_1^2 + g_2^2) = \frac{|\Omega| |\bar{g}|^2}{M}. \quad (6.15)$$

Similarly we obtain

$$d(x) = \frac{|\Omega|}{M} \left( g_2 \left( \frac{\partial u}{\partial x_1}(x) - g_1 \right) - g_1 \left( \frac{\partial u}{\partial x_2}(x) - g_2 \right) \right).$$

We want to estimate

$$\begin{aligned} z^* - \bar{x} &= \int_{\Omega} x c(x) dx - \frac{1}{|\Omega|} \int_{\Omega} x dx + \int_{\Omega} x^{\perp} d(x) dx \\ &= \int_{\Omega} x \left( c(x) - \frac{1}{|\Omega|} \right) dx + \int_{\Omega} x^{\perp} d(x) dx \\ &= \frac{|\Omega|}{M} \int_{\Omega} x \left( g_1 \left( \frac{\partial u}{\partial x_1}(x) - g_1 \right) + g_2 \left( \frac{\partial u}{\partial x_2}(x) - g_2 \right) \right) dx \\ &\quad + \frac{|\Omega|}{M} \int_{\Omega} x^{\perp} \left( g_2 \left( \frac{\partial u}{\partial x_1}(x) - g_1 \right) - g_1 \left( \frac{\partial u}{\partial x_2}(x) - g_2 \right) \right) dx \\ &= \frac{|\Omega|}{M} \int_{\Omega} X G^T (\nabla u(x) - \bar{g}) dx, \end{aligned}$$

where  $X = [x \ x^{\perp}]$  and  $G = [\bar{g} \ \bar{g}^{\perp}]$  are  $2 \times 2$  matrices. Denoting by  $\|\cdot\|$  the spectral norm in  $\mathbb{R}^{2 \times 2}$  it follows that

$$|z^* - \bar{x}| \leq \frac{|\Omega|}{M} \int_{\Omega} \|X\| \|G\| |\nabla u(x) - \bar{g}| dx = \frac{|\Omega|}{M} |\bar{g}| \int_{\Omega} |x| |\nabla u(x) - \bar{g}| dx.$$

Inserting the assumption (6.14), as well as (6.15), we thus conclude that

$$|z^* - \bar{x}| \leq \epsilon \frac{|\Omega|}{M} |\bar{g}|^2 \int_{\Omega} |x| dx = \epsilon \frac{1}{|\Omega|} \int_{\Omega} |x| dx = \omega \epsilon,$$

as was to be shown.  $\square$

Theorem 6.1 shows that the distance between the location computed by the effective dipole method and the center of mass of  $\Omega$  is bounded by the maximal relative error in  $\Omega$  between the spatially varying gradient and its mean. Unfortunately, we do not know how to compute or estimate this error (6.14), neither a priori nor a posteriori. Accordingly, Theorem 6.1 only provides qualitative information about the computed location  $z^*$ .

For the ease of completeness, we state another error estimate that may be more appropriate to use in certain contexts.

**THEOREM 6.2.** *Assume that  $\nabla u(x)$  belongs for all  $x \in \Omega$  to some closed quarter plane  $Q$  rotated around the origin. If  $\delta$  denotes the radius of the circumcircle of  $\Omega$  then there holds*

$$d(z^*, \Omega) \leq \sqrt{2} \delta,$$

where  $d(z^*, \Omega)$  is the Hausdorff distance between  $\Omega$  and the location  $z^*$  of the effective dipole method.

*Proof.* By virtue of our assumptions, we can fix a point  $x^\circ$  such that

$$|x - x^\circ| \leq \delta \quad \text{for all } x \in \Omega.$$

Moreover, in view of the remark following (6.2), we can rotate the coordinate system in such a way that  $Q$  becomes the quarter plane of nonnegative coordinates, i.e., that both components of  $\nabla u$  are nonnegative throughout  $\Omega$  according to the present assumption. Furthermore,  $\nabla u$  cannot vanish identically in  $\Omega$ : Otherwise  $\varphi$  of (3.5) would be zero, and hence,  $u$  would be constant within  $\Omega$ ; using the transmission conditions from (2.3) it would then follow that  $u|_{D \setminus \Omega}$  is a solution of the Cauchy problem

$$\Delta u = 0 \quad \text{in } D \setminus \overline{\Omega}, \quad \frac{\partial u}{\partial \nu} \Big|_{\Gamma} = 0, \quad u|_{\Gamma} = \text{constant},$$

in which case  $u$  would be constant in all of  $D$ , which is a contradiction to  $f \neq 0$ . From this we conclude that (6.13) is nonzero, i.e., that the effective dipole method is well defined.

Using the two identities in (6.12) we obtain from (6.9) that

$$z^* - x^\circ = \int_{\Omega} ((x - x^\circ)c(x) + (x - x^\circ)^\perp d(x)) \, dx,$$

and hence,

$$\begin{aligned} |z^* - x^\circ| &\leq \int_{\Omega} |(x - x^\circ)c(x) + (x - x^\circ)^\perp d(x)| \, dx \\ &= \int_{\Omega} |x - x^\circ| (c^2(x) + d^2(x))^{1/2} \, dx \\ &\leq \delta \int_{\Omega} (c^2(x) + d^2(x))^{1/2} \, dx. \end{aligned}$$

Moreover, by virtue of (6.10) and (6.11), we can rewrite

$$c^2(x) + d^2(x) = \frac{1}{M} |\nabla u(x)|^2,$$

and conclude that

$$|z^* - x^\circ| \leq \delta \frac{1}{\sqrt{M}} \int_{\Omega} |\nabla u(x)| \, dx.$$

Making use of the two inequalities

$$2M \geq \left( \int_{\Omega} \frac{\partial u}{\partial x_1}(x) \, dx + \int_{\Omega} \frac{\partial u}{\partial x_2}(x) \, dx \right)^2,$$

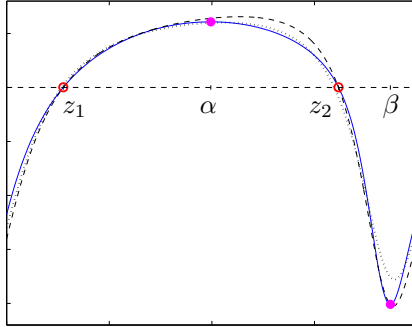


FIG. 7.1. *Boundary potential and approximating dipole potentials.*

and

$$|\nabla u(x)| \leq \frac{\partial u}{\partial x_1}(x) + \frac{\partial u}{\partial x_2}(x), \quad x \in \Omega,$$

where the latter one holds true because  $\partial u/\partial x_1$  and  $\partial u/\partial x_2$  are both assumed to be nonnegative in  $\Omega$ , we finally obtain that

$$|z^* - x^\circ| \leq \sqrt{2} \delta \frac{1}{\sqrt{2M}} \left( \int_{\Omega} \frac{\partial u}{\partial x_1}(x) dx + \int_{\Omega} \frac{\partial u}{\partial x_2}(x) dx \right) \leq \sqrt{2} \delta,$$

which was to be shown.  $\square$

Both theorems establish that the location of the effective dipole method is useful, i.e., close to the convex hull of  $\Omega$ , when the current flows in essentially uniform direction through the inclusion  $\Omega$ . This observation is in favor of low frequent boundary currents like the ones from (3.1) considered in [14], but also in favor of very localized dipole type currents. When the boundary currents are strongly oscillating then currents may flow in various directions through  $\Omega$ , and the error bounds and the computed locations can deteriorate. This is in good agreement with the numerical results shown in Figure 5.2.

**7. Comparison with ad hoc location methods.** In [9, p. 31], Lionheart, Polydorides, and Borsic provide an intuitive argument to locate the inclusion  $\Omega$  from the zeros of the relative data,  $g_0 - g$ , when  $D$  is the unit disk. Note that in this case the relative data essentially coincide with the trace of  $H$ , cf. (3.7).

Lionheart, Polydorides, and Borsic start from the assumption that the difference between  $u$  and the reference potential  $u_0$  behaves like the potential of some dipole located in  $\Omega$ . To illustrate this assumption consider the three graphs in Figure 7.1, in which the solid line depicts the given relative data, i.e., the boundary potential  $g_0 - g$  for the example corresponding to the right-hand side plot in Figure 5.2 with boundary current  $f(t) = \sin 4t$ . The other two graphs are boundary values of dipole potentials: The dotted line represents the effective dipole potential determined in the previous sections, and the dashed line is the dipole potential determined from the zeros  $z_{1/2}$  and the two extrema  $\alpha$  and  $\beta$  of the given relative data.

In the following we will focus on the latter, and describe our geometric construction of the center and the moment of this dipole, which is outlined in Figure 7.2. The

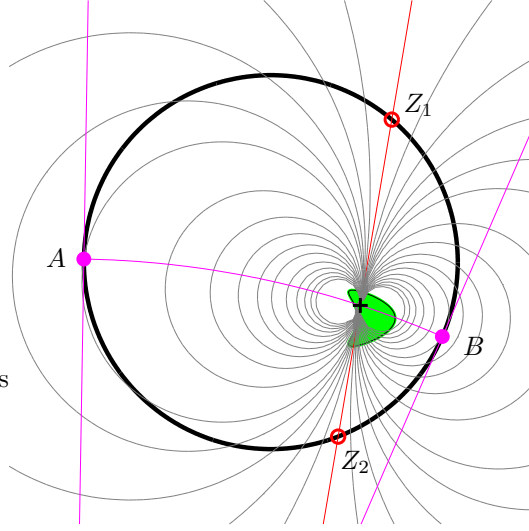


FIG. 7.2. Geometric determination of a suitable dipole potential, and the corresponding level lines.

four points  $A$ ,  $B$ ,  $Z_1$ , and  $Z_2$  in Figure 7.2 correspond to the four polar angles  $\alpha$ ,  $\beta$ ,  $z_1$ , and  $z_2$  from Figure 7.1, and thus mark the two global extrema and the two zeros of the relative boundary data, respectively. Following [9] we assume that the center of the dipole is lying on the straight line connecting the two zeros  $Z_{1/2} \in T$  of  $g_0 - g$ ; this straight line should be orthogonal to the dipole moment  $p$ . Furthermore, for a true dipole potential the dipole is also sitting on a circle connecting the two extrema of  $g_0 - g$ ; the center  $C$  of this circle (not shown on this plot) is the intersection of the two tangents of the unit disk through  $A$  and  $B$ . If the relative data are the boundary values of an exact dipole potential then  $C$  would also lie on the extended line through  $Z_1$  and  $Z_2$ .

How is this geometric location method related to the other two methods described in the previous sections? Well, first of all we have to clarify that within  $D$  the potential  $u_0 - u$  cannot be approximated by a dipole potential, as  $u_0 - u$  must have vanishing flux on the boundary of  $D$ . However,  $u_0 - u$  can behave like a directional derivative of the Neumann function for the Laplacian, cf. Cedio-Fengya, Moskow, and Vogelius [2] for a rigorous asymptotic argument to support this latter claim. On the other hand, when  $D$  is the unit disk, the distinction between dipole potentials and derivatives of Neumann functions, or between  $u_0 - u$  and  $H$ , respectively, becomes irrelevant as their boundary values only differ by a factor of two. Therefore the three location search methods do all require or imply, more or less explicitly, that the auxiliary potential  $H$  introduced by Kwon, Seo, and Yoon (and thus the boundary values  $u_0 - u$  on  $T$ ) can well be approximated by the potential of a dipole located near the center of the inclusion. For the effective dipole method this is the case, for example, if the gradient of  $u$  is almost constant within the inclusion, cf. Theorem 6.1. The location search method requires in addition that the imposed boundary current is of the type (3.1), and that the associated dipole moment  $p$  is very close to the associated vector  $a$  from (3.1); this becomes clear from looking at the equipotentials in Figure 7.2. The other two methods do not require such an assumption, as becomes evident from Figures 5.2 and 7.1, however, the geometric location method is only applicable after a conformal

transformation of  $D$  (and the given data) onto the unit disk. The computed locations of the effective dipole method have been shown to be very accurate, and even best in most of our examples.

**8. Conclusions.** We have compared three methods for the location of inclusions within some homogeneous background material using only one pair of current/voltage measurements on the boundary. We have developed arguments to support our claim that the new effective dipole method is the most efficient and the most reliable among these methods: It requires very little prerequisites, uses a simple and well-defined formula for computing the corresponding location, and this location is often found to be close to the center of mass of the inclusion. The error bounds that we have obtained can be used to justify our numerical findings.

#### REFERENCES

- [1] K. BRYAN, Numerical recovery of certain discontinuous electrical conductivities, *Inverse Problems*, 7:827–840, 1991.
- [2] D. J. CEDIO-FENGYA, S. MOSKOW, AND M. S. VOGELIUS, Identification of conductivity imperfections of small diameter by boundary measurements. Continuous dependence and computational reconstruction, *Inverse Problems*, 14:553–595, 1998.
- [3] H. HAKULA AND N. HYVÖNEN, Two noniterative algorithms for locating inclusions using one electrode measurement of electric impedance tomography, submitted.
- [4] M. HANKE, N. HYVÖNEN, M. LEHN, AND S. REUSSWIG, Source supports in electrostatics, submitted.
- [5] M. HANKE, N. HYVÖNEN, AND S. REUSSWIG, Convex source support and an algorithm for approximating inhomogeneities using one measurement of electrical impedance tomography, in preparation.
- [6] F. HETTLICH AND W. RUNDELL, The determination of a discontinuity in a conductivity from a single boundary measurement, *Inverse Problems*, 14:67–82, 1998.
- [7] K. ITO, K. KUNISCH, AND Z. LI, Level-set function approach to an inverse interface problem, *Inverse Problems*, 17:1225–1242, 2001.
- [8] O. KWON, J. R. YOON, J. K. SEO, E. J. WOO, AND Y. G. CHO, Estimation of anomaly location and size using electrical impedance tomography, *IEEE Trans. Biomed. Eng.*, 50:89–96, 2003.
- [9] W. LIONHEART, N. POLYDORIDES, AND A. BORSIC, *The reconstruction problem*, Chapter 1 in *Electrical Impedance Tomography: Methods, History and Applications*, D. Holder, ed., IOP Publishing, Bristol, 2005, pp. 3–64.
- [10] H. KANG, J. K. SEO, AND D. SHEEN, Numerical identification of discontinuous conductivity coefficients, *Inverse Problems*, 13:113–123, 1997.
- [11] R. KRESS, *Linear Integral Equations*, 2nd ed., Springer, Berlin, 1999.
- [12] R. KRESS AND W. RUNDELL, Nonlinear integral equations and the iterative solution for an inverse boundary value problem, *Inverse Problems*, 21:1207–1223, 2005.
- [13] O. KWON AND J. K. SEO, Total size estimation and identification of multiple anomalies in the inverse conductivity problem, *Inverse Problems*, 17:59–75, 2001.
- [14] O. KWON, J. K. SEO, AND J.-R. YOON, A real-time algorithm for the location search of discontinuous conductivities with one measurement, *Comm. Pure Appl. Math.*, 55:1–29, 2002.
- [15] J. SYLVESTER, Notions of support for far fields, *Inverse Problems*, 22:1273–1288, 2006.